═══REVIEW COMMONS MANUSCRIPT═══

IMPORTANT:

- Manuscripts submitted to Review Commons are peer reviewed in a journal-agnostic way.
- Upon transfer of the peer reviewed preprint to a journal, the referee reports will be available in full to the handling editor.
- The identity of the referees will NOT be communicated to the authors unless the reviewers choose to sign their report.
- The identity of the referee will be confidentially disclosed to any affiliate journals to which the manuscript is transferred.

GUIDELINES:

- For reviewers: https://www.reviewcommons.org/reviewers
- For authors: https://www.reviewcommons.org/authors

CONTACT:

The Review Commons office can be contacted directly at: office@reviewcommons.org

Endocytosis of the plasma membrane carboxylate transporter Jen1 in *Saccharomyces cerevisiae* under alkali stress: a mechanism for preventing loss of essential metabolites

Cláudia Barata-Antunes[1,2], Erik de Hulster[3], Clara Cardoso[3], Inês P. Ribeiro[1,4], Vítor Fernandes[1,2], Beatriz Leite[1,2], Margarida Casal[1,2], Hernâni-Gerós[1,5,6], Jack Pronk[3], Joaquín Ariño[7], Robert Mans[3], Sandra Paiva[1,2]

[1]Centre of Molecular and Environmental Biology, Department of Biology, University of Minho, 4710-057, Braga, Portugal
[2]Institute of Science and Innovation for Bio-Sustainability (IB-S), University of Minho, 4710-057, Braga, Portugal
[3]Department of Biotechnology, Delft University of Technology, Van der Maasweg 9, 2629 HZ, Delft, The Netherlands
[4]Life and Health Sciences Research Institute (ICVS), University of Minho, Braga, Portugal
[5]Centre for the Research and Technology of Agro-Environmental and Biological Sciences, University of Trás-os-Montes and Alto Douro, Vila Real, Portugal
[6]Centre of Biological Engineering (CEB), Department of Biological Engineering, University of Minho, Braga, Portugal
[7]Institut de Biotecnologia i Biomedicina & Departament de Bioquímica i Biologia Molecular, Universitat Autònoma de Barcelona, Cerdanyola del Vallès, Spain

Correspondence:
Sandra Paiva: spaiva@bio.uminho.pt
Robert Mans: robert.mans89@gmail.com

Abstract

When grown on lactate as a sole carbon source, *Saccharomyces cerevisiae* cells alkalinize their surroundings. This alkalinization coincides with endocytosis of the Jen1 lactate transporter. Previous studies showed that this process depends on a functional Jen1 transporter and involves Bul1 α-arrestin and an active TORC1 complex. However, it remained unclear whether the internalization of Jen1 triggered by prolonged growth on lactate was exclusively due to the increase in external pH. To further investigate the regulatory mechanisms underlying the alkali stress-induced Jen1 endocytosis, *S. cerevisiae* cells stably expressing a *JEN1-GFP* fusion were studied in aerobic carbon-limited continuous cultures subjected to a linear increase of the culture pH. We found that, in these controlled bioreactor cultures, Jen1 internalization is strongly dependent on extracellular pH, showing a sharp transition at pH values of 7.0 to 7.2. This pH threshold coincides with wash-out of the chemostat cultures and with release of pyruvate and acetate. Transcriptome analysis revealed upregulation of genes involved in oxidative phosphorylation around this threshold, which is consistent with higher cellular energy requirements or energy metabolism being compromised. The originality of this study lies in the use of continuous cultures to analyse the endocytosis of a yeast nutrient transporter. This approach allowed the rigorous study of cell responses to a specific alteration in a single environmental condition, such as changes in pH.

Keywords: transporters; carboxylic acids; endocytosis; alkali stress; lactate, pH, chemostat cultivation.

1. Introduction

In nature, *Saccharomyces cerevisiae* cells continuously face changes in their surroundings, such as nutrient fluctuations and stress conditions. To adapt to these challenges, cells are able to reprogram their metabolism by inducing or repressing the transcription of specific genes [1–4]. In addition, they respond at a post-translational level by promoting the internalization (endocytosis) and degradation of plasma membrane (PM) transporters that can be deleterious or dispensable under those conditions [5–7].

Jen1 is a transmembrane proton-symporter of the yeast *S. cerevisiae* that transports the monocarboxylates lactate, pyruvate, acetate and propionate together with a proton (H^+) [8–11]. Jen1 was also reported to transport selenite [12] and it is expressed and localized at the PM when cells are growing on non-fermentable carbon sources, including lactate, pyruvate, acetate and ethanol [13]. A variety of signals induce Jen1 internalization and degradation, including glucose [10, 14–20], rapamycin, and cycloheximide ([21], see also [5] for a review). In our recent study [21], we found that yeast cells growing on lactate or pyruvate alkalinize their surroundings from an initial pH of 5.0 to around 7.0. This final near-neutral pH coincides with Jen1 endocytosis and degradation [21]. Moreover, we showed that the Bul1 arrestin (an adaptor of Rsp5 ubiquitin ligase), an active TORC1 complex, and ammonium (a preferable nitrogen source), are necessary for efficient pH dependent endocytosis of Jen1 [21]. However, the regulatory networks that connect external pH alkalinization to Jen1 downregulation remain elusive.

In shake-flask cultures, dynamic changes in extracellular pH, organic acid concentration and other growth conditions are highly dynamic. These changes affect gene expression [22] and other intracellular processes, including endocytosis of proteins localized at the PM. In such simple cultivation systems, relevant changes in gene expression specifically related to Jen1 endocytosis are difficult to identify. In contrast, in well-mixed continuous cultures at steady state, cells can be grown under the same conditions for prolonged periods of time. Furthermore, key culture parameters can be maintained at preferred setpoints and be controlled independently, including specific growth rate, temperature, biomass concentration, pH, and oxygen availability [23]. The use of continuous cultures therefore facilitates the identification of genes that specifically respond to a single environmental condition (e.g.,

extracellular pH), because other culture parameters, including the specific growth rate, can be kept constant.

The plasma membrane ATPase (Pma1) of *S. cerevisiae* cells generates an electrochemical proton gradient, the proton motive force (pmf), across the PM by pumping out a proton at the expense of ATP [24]. This proton motive force consists of the pH gradient ($\Delta pH = pH_{in} - pH_{out}$) and the electrical potential difference resulting from the charge gradient, generated by the movement of positive or negative charges to the extracellular space ($\Delta\psi = \psi_{in} - \psi_{out}$, in V) [25]. Because Jen1 is an electroneutral monocarboxylate/proton symporter, with a stoichiometry of 1 H^+ (proton): 1 monocarboxylate (anion) [10], only the pH gradient (ΔpH) can energizes monocarboxylate uptake against its concentration gradient [25] and determines the accumulative capacity of the symporter (see equations and **Table S1** in supplementary data). In addition to its role in monocarboxylate uptake, Jen1 has also been implicated in monocarboxylate export [26–29], which indicates that this transporter functions bidirectionally. Therefore, when monocarboxylate concentrations across the membrane are equal and the external pH becomes higher than the internal pH and the driving force for proton-coupled monocarboxylate transport is outward, Jen1 could function as an exporter. We hypothesise that under these conditions, the Jen1 transporter is internalized and removed from the PM to avoid 'leakage' of lactate and other organic acids (**Fig. 1A**). To test this hypothesis and to identify the regulatory mechanisms underlying Jen1 endocytosis, *S. cerevisiae* cells stably expressing *JEN1* fused to GFP were grown in aerobic, carbon-limited continuous cultures on a mixture of ethanol and lactate at extracellular pH values below and above the assumed near-neutral cytosolic pH [30–33]. Using this experimental set-up, we determined Jen1 localization, the extracellular concentration of Jen1-transported metabolites, and the transcriptome profiles at different extracellular pHs. Our results indicate that when an external pH of 7.0 is exceeded, key metabolites are lost while Jen1 is largely internalized and that this is accompanied by transcriptional remodelling, seemingly aimed to improve respiratory capacity. These findings support the hypothesis that Jen1 internalization is a response to minimize the loss of essential metabolites when environmental pH surpasses intracellular pH.

2. Results

2.1. Aerobic, carbon-limited continuous cultivation with a linearly increasing culture pH

In order to determine the threshold value of the external pH at which internalization of the Jen1 transporter occurs, aerobic, carbon-limited continuous cultures of *S. cerevisiae* [34] stably expressing Jen1 fused to GFP (Jen1-GFP) were grown on a synthetic medium with lactic acid and ethanol as carbon sources, at pH 6.5 (see Material and Methods for details). After a steady state was reached, a 'pH ramp' was programmed, during which the pH of the external medium was gradually increased from pH 6.5 to 7.5 at a rate of 0.02 pH units h^{-1}. Different parameters were monitored along the experiment, including CO_2 and O_2 concentrations in the exhaust gas, biomass, the concentration of extracellular metabolites, and the subcellular localization of Jen1-GFP (**Fig. 1A-E**). With this approach, we aimed to define the pH at which Jen1 is internalized and to investigate the physiological consequences of this internalization. Since Jen1 is the predominant lactate import system in *S. cerevisiae* [8, 9], we anticipated that this pH threshold should coincide with a severe reduction of lactate import. With the objective to enable growth of the continuous cultures even when lactate would no longer be transported, ethanol was used as co-substrate.

Fluorescence microscopy (**Fig. 1C**) revealed that the Jen1-GFP signal was clearly localized at the PM at culture pH values of 6.5, 6.75 and 7.0. However, a further increase in the external pH resulted in a decreased fluorescence signal at the cell periphery. When the external pH reached values equal to or above 7.25, Jen1-GFP was no longer observed at the PM and instead was predominantly localized at the vacuole. This observation was supported by the quantification of the ratio of the fluorescence at the PM over the total fluorescence, which decreased from 0.42 ± 0.091 (mean ± s.d.) at pH 6.75 to 0.18 ± 0.077 at pH 7.5 (**Fig. 1D**). At pH values of 7.25 and above, cells were unable to maintain a sufficiently high growth rate to keep up with the dilution rate of the continuous cultures (0.07 h^{-1}). The resulting progressive wash-out of biomass was accompanied by a steep decrease of the CO_2 concentration in the bioreactor off gas and a corresponding increase in the off-gas O_2 concentration (**Fig. 1B**).

The residual concentration of lactate in continuous cultures did not significantly change between pH 6.5 and 7.0 (**Fig. 1E** and **Table S2**). However, above pH 7.0, the

lactate concentration steeply increased from 9 ± 1 mg/L (mean ± s.d.) to 495 ± 101 mg/L at pH 7.5. No extracellular ethanol was detected when cultures were grown at pH values between 6.5 and 7.25, but at pH 7.5 an extracellular concentration of 0.36 ± 0.07 g L^{-} ethanol was measured, coincident with a decrease in biomass dry weight (**Table S3**). These results clearly show that the threshold extracellular pH at which Jen1-GFP is removed from the PM lies between pH 7.0 and 7.2.

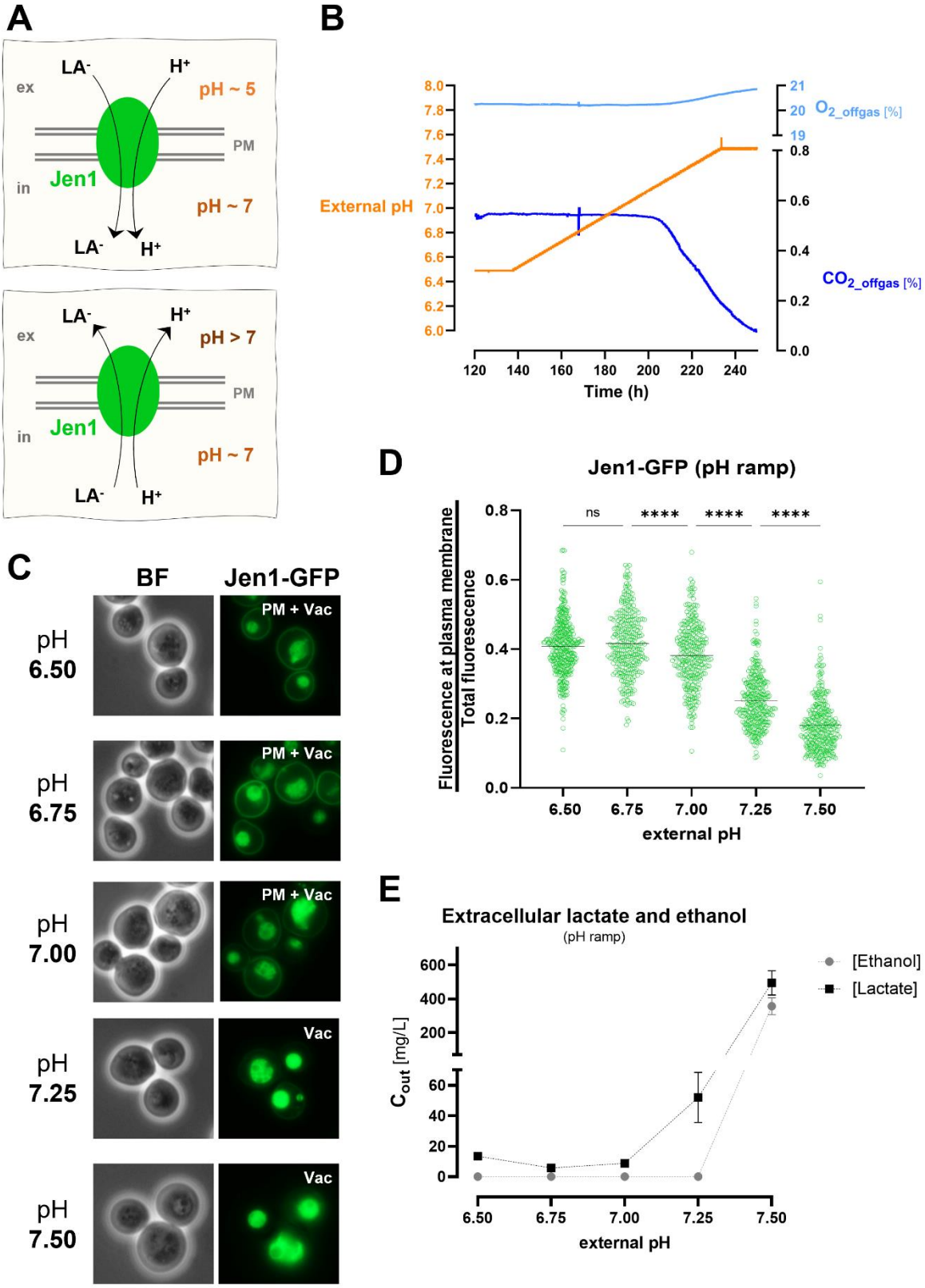

Fig. 1 Evaluation of Jen1-GFP localization and other parameters (off-gas CO_2 and O_2 concentrations, extracellular concentration of lactate and ethanol) using a pH ramp approach in aerobic-, carbon- limited continuous *S. cerevisiae* cultures.
Cells were grown in SM containing 50 mM ethanol and 30 mM lactic acid as carbon sources, at a dilution rate of 0.07 h^{-1}. Culture pH was controlled by the automated addition of 2 M KOH or 2 M H_2SO_4 (see Material and

Methods). **(A)** Schematic representation of the flux direction of lactate anions (La^-) and protons (H^+) through the Jen1 transporter under different extracellular pHs and identical La^- concentrations in- and outside of the cells. At extracellular pHs near 5 and considering the pH of the cytosol near 7 [30–33], the driving force is inward and La^- is accumulated inside the cell. In contrast, at extracellular pHs above 7, the driving force is outward and, consequently, La^- is exported. **(B)** Values for CO_2 and O_2 concentration (%) in the outflow gas were monitored simultaneously with the progressive increase (0.1 units each 5 h) of the external pH from 6.5 to 7.5. **(C)** Cells were visualized by epifluorescence microscopy at the specific extracellular pHs indicated (pH 6.5, 6.75, 7.0, 7.25 and 7.5). The primary localization of the Jen1-GFP is described at the top left corner of each fluorescence microscopy image. PM, plasma membrane; Vac, vacuole; BF, bright field. **(D)** At the indicated pHs, quantifications of the ratio of the fluorescence at the plasma membrane over the total fluorescence were made (see Material and Methods). The data is represented as a scatter plot with median (n≥300 cells). ns, not significative: $P>0.05$; ****$P<0.0001$ (ordinary one-way ANOVA analysis was used followed by a Tukey's multiple comparisons test. (E) Extracellular concentrations of ethanol and lactate are expressed in mg of substrate (lactate or ethanol) per L of the culture medium.

2.2 Studies in steady-state cultures at specific extracellular pH values

To establish steady-state cultures at specific pH values, individual bioreactors were programmed at the following pH values: pH 6.0 and 6.5 (Jen1 still at the PM), pH 7.0 and 7.1 (values close to the Jen1 internalization threshold pH identified above) and pH 7.2 (Jen1 largely removed from the PM). Once cultures had reached steady state at each of the selected pH values, culture samples were taken for measurements of biomass, for microscopy and for transcriptomic analysis. Under these stable steady-state culture conditions, at pHs 6.0 and 6.5, Jen1-GFP (**Fig. 2B**) localized both at the PM and at the vacuole, while at the extracellular pH 7.0 or 7.1, the amount of Jen1-GFP at the PM decreased abruptly and the fluorescence signal at the vacuole increased. Consequently, the PM/total fluorescence ratio decreased from 0.51 ± 0.07 (pH 6.0) to around 0.31 at pHs 7.0 and 7.1 (**Fig. 2C**).

Over the evaluated range of culture pH values, no ethanol was detected in culture supernatants, which is consistent with the carbon-limited cultivation regime. In contrast, the residual concentration of lactate in the cultures, which was around 13 mg/L at pH 6.0 and 6.5, and increased only moderately at pH 7.0, raised abruptly to 92 mg/L at pH 7.1 (**Fig. 2D**; see also **Table S4**).

Cultures growing at pH values above 7.0, as well as their culture supernatants, changed colour from beige to orange/brown (see schematic representation in **Fig. 2A**). This phenomenon was also observed after prolonged (over 24 h) growth in shake-flask cultures on SM with lactic acid as sole carbon source (data not shown). The cause of this colour change is unknown but merits further investigation.

Notably, in continuous cultures grown at pH values above 7.1, cells were unable to sustain a growth rate equal to the dilution rate (0.07 h^{-1}) and, consequently, washout

occurred. We therefore could not establish steady-state cultures at pH 7.2, at which Jen1 is likely fully localized at vacuoles (**Fig. 1C**).

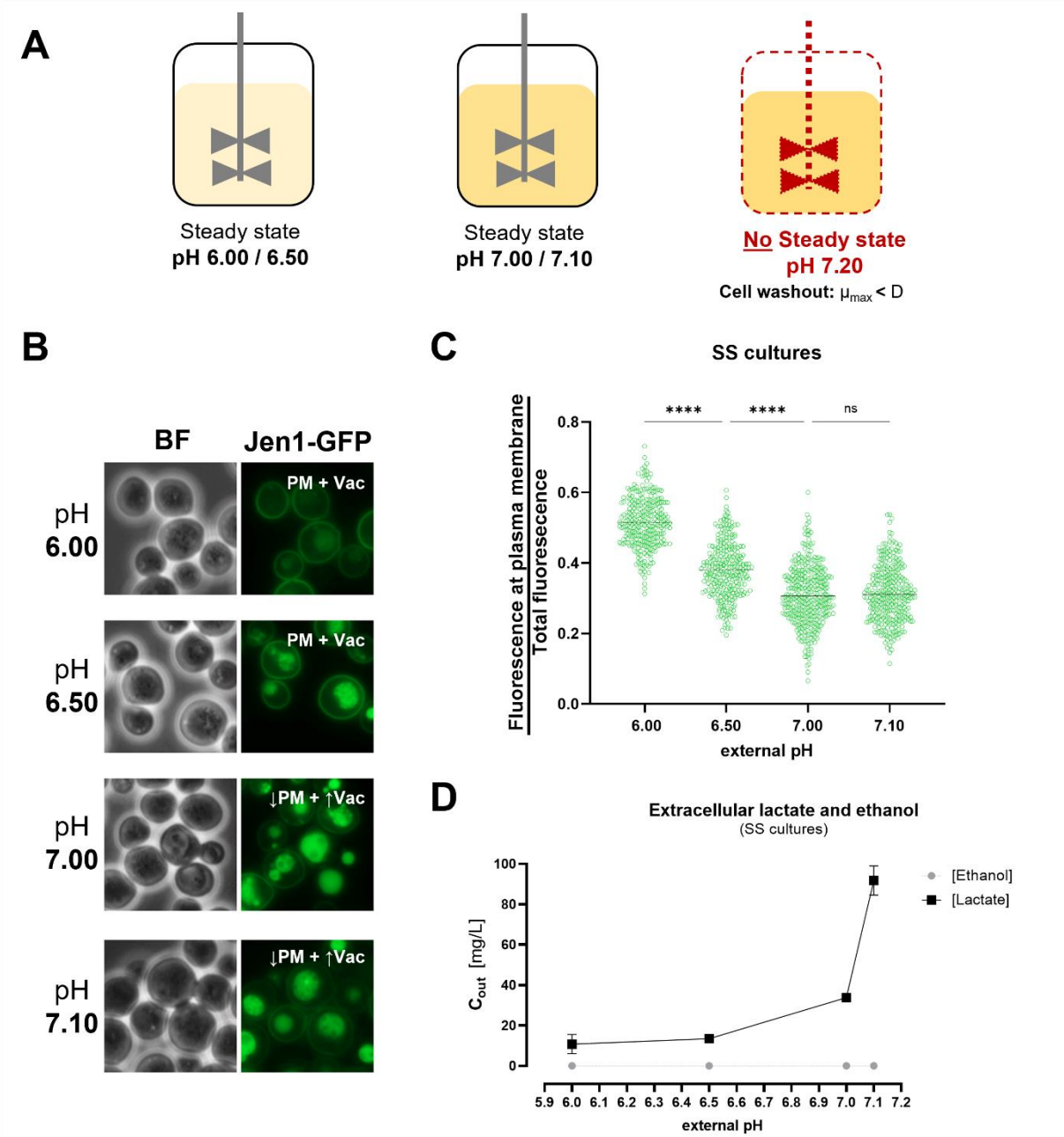

Fig. 2 Analysis of Jen1 localization and of other physiological parameters using steady state (SS) continuous cultures growing aerobically and programmed at specific and relevant pHs. **(A)** Schematic representation of the bioreactors used to run the continuous cultures set up at pH 6.0, pH 6.5, pH 7.0, pH 7.1 and 7.2. At pHs above 7.0, the culture media changed the colour from beige to orange/light brown. At extracellular pH of 7.2, the cells grew at a specific growth rate (μ) lower than the set dilution rate (D = 0.07 h^{-1}), which caused cell washout. Cells were grown in SM containing 50 mM ethanol and 30 mM lactic acid as carbon sources, at a dilution rate of 0.07 h^{-1}. Culture pH was maintained at 6.0, 6.5, 7.0, 7.1 or 7.2 by the automated addition of 2 M KOH or 2 M H_2SO_4 (see Material and Methods). **(B)** When the cultures reached the steady state, cells were visualized by epifluorescence microscopy. The primary localization of the Jen1-GFP is described at the top left corner of each fluorescence microscopy image. PM, plasma membrane; Vac, vacuole; BF, bright field. **(C)** Quantifications of the ratio of the fluorescence at the plasma membrane over the total fluorescence

were made (see Material and Methods). The data is represented as a scatter plot with median (n≥270 cells). ns, not significative: P>0.05; ****P<0.0001 (ordinary one-way ANOVA analysis was used followed by a Tukey's multiple comparisons test. **(D)** Extracellular concentrations of ethanol and lactate are expressed in mg of substrate (lactate or ethanol) per L of the culture medium.

Besides lactate, also pyruvate, acetate, succinate, citrate, and glycerol were determined in culture supernatants of each steady-state culture (**Fig. 3A**, **Table S5**). Whereas between pHs 6.0 and 7.0, few changes were observed in the concentrations of these metabolites, pyruvate and acetate concentrations were 7- to 9-fold higher in cultures grown at pH 7.1 than in cultures grown at pH 7.0.

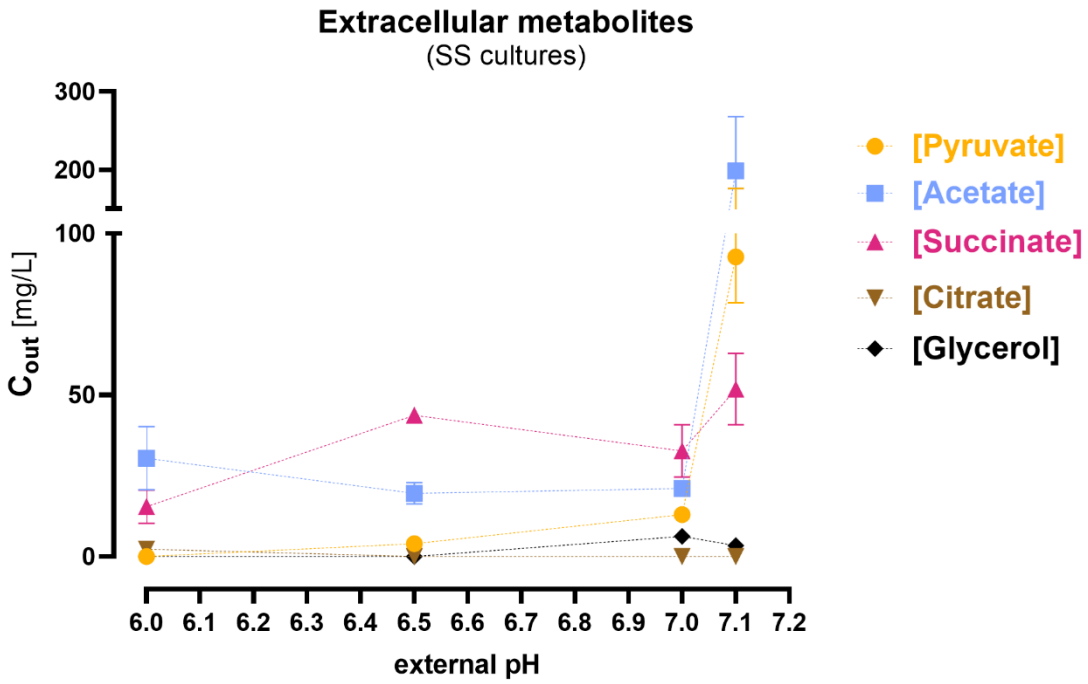

Fig. 3 Determination of extracellular metabolites produced in steady state, aerobic, continuous cultures of *S. cerevisiae* growing in SM with ethanol and lactate and set up at different extracellular pHs. The concentration values are expressed as mg of substrate per L of culture medium. Cells were grown in SM containing 50 mM ethanol and 30 mM lactic acid as carbon sources, at a dilution rate of 0.07 h^{-1}. The culture pH was maintained at 6.0, 6.5, 7.0, 7.1 or 7.2 by the automated addition of 2 M KOH or 2 M H_2SO_4 (see Material and Methods). The values are the mean of at least two independent experiments (n≥2).

2.3 Transcriptome sequencing (RNA-seq) analysis of steady state-, aerobic-, continuous cultures of *S. cerevisiae* set up at different extracellular pH values

Samples of steady-state, aerobic continuous cultures of *S. cerevisiae* grown at pH values of pH 6.0, 6.5, 7.0, and 7.1 were used for RNA sequencing. The RNA-seq analysis data was combined, and comparisons were made between the datasets obtained at the different pH values. As expected, the effect on gene expression was

related to the intensity of the pH stress. The increase of pH from 6.0 to 6.5 affected a relatively small number of genes, barely above 100 (most of them induced, **Fig. 4**). A further increase of the culture pH to 7.0 resulted in a higher number of genes with altered expression levels, with a particular increase in the number of those whose mRNA decreased. Interestingly, a relatively small increase of the culture pH by 0.1 units (7.1vs6.0 in comparison with 7.0vs6.0) doubled the number of mRNAs that were altered, with a nearly 3-fold increase in the number of repressed genes. It is worth noting that a significant number of genes (more than 100) was also affected when data at pH 7.1 was compared with that obtained at 7.0 (**Fig. 4A**).

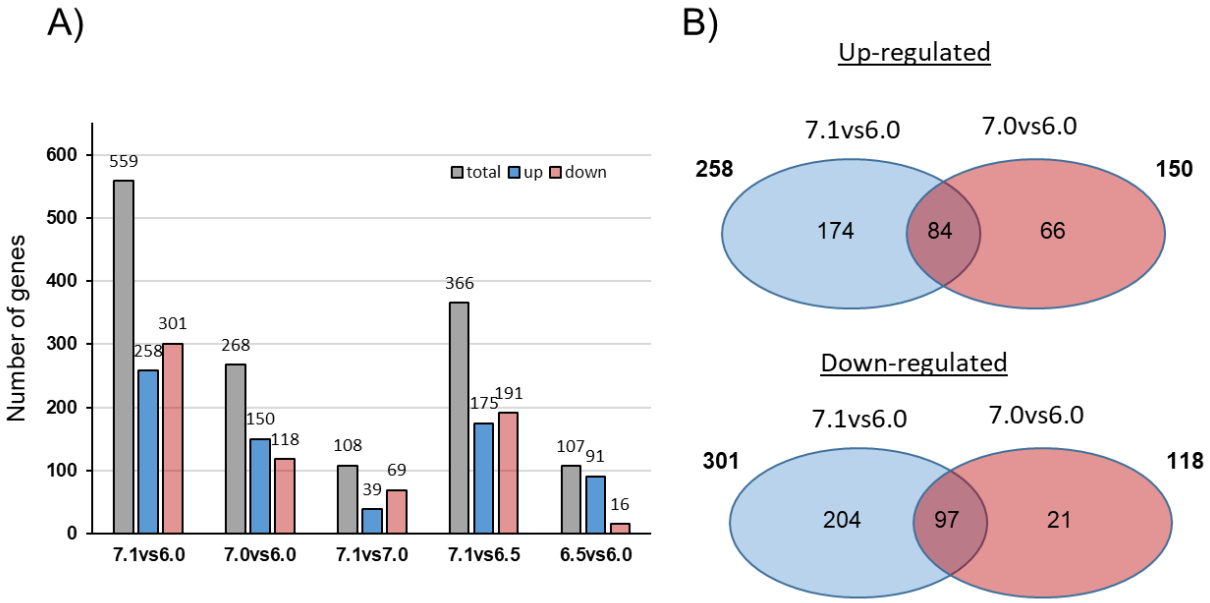

Fig. 4 Transcriptional impact of external pH in steady state, continuous cultures of *S. cerevisiae*. Cells were grown in SM (ethanol plus lactate) in aerobic-, continuous- cultures set up at different pHs (pH 6.0, 6.5, 7.0 and 7.1). **(A)** Different pH groups were compared (6.5vs6.0; 7.0vs6.0; 7.1vs6.0; 7.1vs6.5 and 7.1vs7.0). The grey column represents the total number of altered genes, and the blue and orange columns represent the number of up-regulated or down-regulated genes, respectively. **(B)** Venn diagrams of differentially expressed genes (DEG) for the pH 7.1vs6.0 and 7.0vs6.0 data sets. Number of genes in each dataset are denoted in bold outside the ovals. The overlapping region indicates the numbers of differentially expressed genes that are common in the compared groups.

The transition from pH 6.0 to pH 7.0 or 7.1 resulted in changes consistent with previously reported data from cells subjected to mild alkalinization (see Discussion). Thus, diverse genes related to iron uptake and metabolism (*SIT1*, *FIT2*, *FIT3*, *FRE1*, *FET3*, and *HXM1*), high-affinity phosphate (*PHO84*, *PHO89*), or hexose transport (*HXT14*, *HXT10*, *HXT2*) were induced by the shift to either pH 7.0 or 7.1 (**Fig S1**). **Figure 4B** shows the overlap between the largest set of up-regulated or down-regulated genes (the comparison between pH 7.1 and 6.0) and the 7.0vs6.0 data set.

It is worth noting that 174 of the 258 genes (59.7%) induced when comparing pH 7.1 and 6.0 were not found to be induced when comparing pH 7.0 and 6.0, whereas 204 out of 301 (67.8%) were found repressed in the former case but not in the latter. This suggests that the transition from pH 7.0 to pH 7.1, albeit it might appear quantitatively minor, has a significant impact in the expression profile of the cells. Since the most significant internalization of Jen1 seemed to be triggered by events during this transition, we found it pertinent to further examine the 174 genes specifically induced in cells exposed to the pH change from 6.0 to 7.1, but not from 6.0 to 7.0.

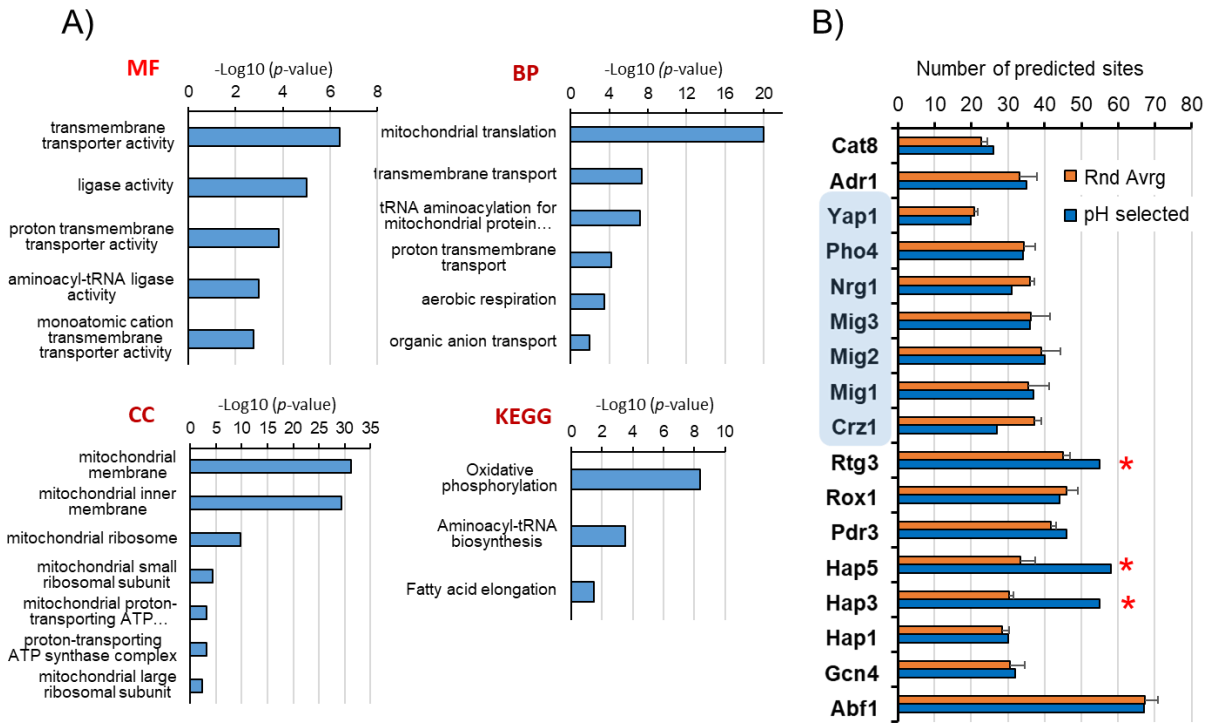

Fig. 5 Gene Ontology and promoter analysis of the 174 genes specifically induced at the pH 6.0 to 7.1 transition. (A) The GO terms of the MF (Molecular Function), BP (Biological Process), and CC (Cellular component) domains enrichment of the 174 differentially expressed (up-regulated) genes. GO, Gene Ontology; KEGG, Kyoto Encyclopaedia of Genes and Genomes biological pathways database. The *p*-value threshold was set at 0.05. **(B)** The JASPAR database matrices were used to scan for transcription factor binding sites in the promoters of the mentioned genes (pH selected). As reference, four sets of 174 randomly selected genes were also scanned and the mean ± SEM of the number of predicted sites is offered for comparison. The asterisks denote binding sites whose abundance is markedly increased in the pH selected gene cohort. The blue shading denotes transcriptions factors whose activity is affected by alkalinization (see discussion).

As shown in **Fig. 5** and **Fig. S2**, this set was strongly enriched for genes related to mitochondrially-related events, with 70 genes (40%) encoding mitochondrial membrane-associated proteins (**Table S6**). Thirty-three genes were directly related to mitochondrial translation, including those encoding ribosomal proteins (such as *MRPL17*, *MRPL3, MRPL10,* and others), translation factors (such as *MRF1*, *MEF1*,

IFM1, or *TUF1*), or RNA aminoacyl ligases (including *SLM5, MSR1, MST1, ISM1* and others). It is worth noting that genes encoding cytosolic ribosomal genes were not induced at all. In addition, sixteen genes were related to oxidative phosphorylation, either as members of the electron transport chain (such as *RIP1*, *SDH3*, *COX6*, *COX10*, *COX11* and others) or as components of the ATP synthase complex (*ATP2*, *ATP4*, *ATP5*, *ATP16*, *ATP17*, and *TIM11*). The promoter region of the 174 genes was investigated for predicted transcription binding sites. As shown in **Fig. 5B**, such promoter regions were not enriched for consensus sequences corresponding to activators or repressors (shaded in blue) known to play a relevant role in the overall adaptation to alkalinization (in fact, a decrease for the calcium-calcineurin activated Crz1 transcription factor was observed). In contrast, an enrichment for Rtg3 and, in particular, for Hap3 and Hap5 was detected. Rtg3 is a positive regulator of the retrograde pathway, which responds to mitochondrial dysfunction by adapting cell metabolism to the loss of tricarboxylic acid (TCA) cycle activity ([35, 36], reviewed in [37]). Hap3 and Hap5 are subunits of the Hap2p/3p/4p/5p CCAAT-binding complex, a transcriptional activator of respiratory gene expression (TCA cycle and oxidative phosphorylation genes) [38, 39]. Interestingly, the minimal change from pH 7.0 to 7.1 resulted in the transcriptional upregulation of 39 genes, of which only four (the permeases *DIP5*, *BAP3*, *GNP1*, and *TAT1*) were also induced in the transition from pH 6.0 to 7.0. Gene Ontology analysis of the 35 non-induced genes yielded a clear enrichment (*p*-value=1.8E-6) in genes encoding components of the mitochondrial inner membrane, thus reinforcing the notion that the transition from pH 7.0 to 7.1 has a significant impact on the regulation of mitochondrial function.

3. Discussion

In this study, we hypothesized that, as the extracellular pH increased above the intracellular pH, the consumption of lactate would cease due to the inversion of the driving force for uptake (see introduction and **Fig. 1A**), but that a steady state could still be achieved via the supplied ethanol. However, at pH 7.2 no steady-state culture could be obtained when a mixture of ethanol and lactate was supplied. Apparently, even though Jen1 was largely internalized at this pH, and the pH-ramp experiment indicated that ethanol could still be efficiently consumed (**Fig. 1E**), this was not sufficient to prevent the growth rate from decreasing below the dilution rate of 0.07 h^{-1}. The modest increase in pH from 7.0 to 7.1 resulted in 7 and 9-fold higher extracellular concentrations of acetate and pyruvate, respectively (**Fig. 3**, **Table S5**). Pyruvate, the product of glycolysis, and acetate, the precursor of cytosolic acetyl-CoA, are key intermediates in the central metabolism of yeast [40] (see **Fig. S3**). Given that these substrates are transported via Jen1 and that, in the case of pyruvate, Jen1 is the only monocarboxylate permease capable of efficiently transporting this substrate in *S. cerevisiae* [41], the cellular leakage of pyruvate is likely via Jen1 export when the transporter is still functional at these pH levels. Diffusion of pyruvic acid (PyrH) (pKa = 2.49) through the PM can be largely excluded because the charged, deprotonated form of pyruvate (Pyr^-) prevails (pKa=2.5) at neutral-alkali pHs [32, 42]. At pH 7.2, loss of these metabolites may have become too high to maintain the set growth rate of 0.07 h^{-1}, which can explain why we were unable to establish a steady-state culture at pH 7.2 in which ethanol was used as carbon and energy source. A similar sharp increase in the extracellular concentration of acetate at neutral pH values was reported previously in glucose-limited cultures of *S. cerevisiae* [43]. Furthermore, weak growth on ethanol at pH values >7 in batch cultures [44] could indicate that growth on this substrate, for which the catabolic pathway has acetate as an intermediate metabolite, could be severely impacted by this form of carbon loss. Our results suggest that, at a high external pH, endocytosis of Jen1, and possibly of other H^+/carboxylate symporters, may be required in order to limit the loss of crucial carbon metabolites by the cells. However, even though Jen1 appeared completely internalized at pH >7.1 (**Fig. 1**), this alone seems insufficient to prevent the loss of these monocarboxylates.

Our transcriptomic data corresponding to the transitions from pH 6.0 to pH 7.0 or 7.1 reveals an increase in mRNA levels of genes involved in iron and copper uptake and metabolism, as well as in high-affinity phosphate and sugar transport. These

changes fit well with previously reported data that different research groups obtained from exponentially growing batch cultures that were subjected to moderate alkalinization [45–47]. However, our data also show that the transition to pH 7.1 triggers a specific response that is not observed in cells shifted from pH 6.0 to 7.0. This response involves induction of genes involved in oxidative phosphorylation (**Fig. 5**) and indicates that the shift to pH 7.1 caused a very specific effect on metabolism-related gene expression. Tu *et al* [48] showed that *S. cerevisiae* cells grown under continuous, nutrient-limited conditions after a short initial starvation period, exhibit highly periodic cycles related to respiratory bursts. They identified three repetitive superclusters, oxidative (Ox), reductive/building (R/B), and reductive/charging (R/C), thus defining three major phases of the yeast metabolic cycle. We soon realized that the top 40 R/B genes showing stronger periodicity included 13 of our 174 genes, whereas none of them appeared in the top 40 Ox or R/C lists. To better quantify this apparently specific correspondence, we performed a cluster analysis with the transcriptomic data reported in [48] for the 149 genes in common with our 174 gene list. As presented in **Figure 6**, with few exceptions all these genes are expressed following the R/B supercluster pattern. As the mentioned R/B supercluster peaks when cells are about to cease oxygen consumption, it could be interpreted as a preparatory step to meet an acute requirement to increase respiratory capacity. It must be noted that the expression of many of the genes identified in the specific switch from pH 6.0 to 7.1 does not seem linked to a general response to alkalinization, as the promoters of these genes are not enriched in binding sites for any of the diverse transcription factors known to shape the alkaline pH response [49]. Instead, such response is clearly connected to the mitochondria, and appear to reflect a first step in intensifying the capacity for mitochondrial respiration. This is reflected in the enrichment in Rtg3 and, specially, Hap3 and Hap5 binding sites in their promoters, as these transcription factors are pivotal components of the adaptation to respiration [39]. Interestingly, an increase in the TCA cycle activity and respiratory rate when batch cultures of yeast cells were switched to pH 7.5 was reported [50].

In summary, the combination of Jen1-GFP localization data, quantitative bioreactor experiments and transcriptome analysis indicate that lactate transport via Jen1 causes immediate cellular stress when the extracellular pH exceeds a threshold value that corresponds to the intracellular (cytosolic) pH [30–33]. Once across this pH threshold, reversal of the driving force for lactate concentration via the Jen1 La^-/H^+

symporter will reverse the thermodynamic driving force for lactate consumption and, thereby, in the absence of an alternative energy substrate, immediately affect cellular energy status. This interpretation is supported by the observed transcriptional upregulation, in cultures subjected to pH values that are above this threshold, of genes involved in synthesis of mitochondrial proteins and, more in particular, genes involved in oxidative phosphorylation. Even when an additional carbon and energy substrate, such as ethanol, is provided, the observed export of the biosynthetic precursors pyruvate and acetate, also substrates of Jen1, create another metabolic burden. These observations support the notion that internalization of Jen1 has evolved as a mechanism that increases cellular robustness to dynamics in environmental pH.

Our data are in line with studies on the *S. cerevisiae* H^+-uracil symporter Fur4, in which a rapid loss of intracellular uracil (~60 %) was also reported under alkali stress conditions [51]. It would be interesting to explore whether similar regulatory processes extend to other H^+/carboxylate symporters in *S. cerevisiae* or to other yeast species. Our study emphasises the importance of the mode of energy coupling (dependence on charge or concentration gradients vs. direct ATP hydrolysis) in transporters in order to increase cellular robustness under dynamic conditions [52]. It also highlights the importance of pH regulation for maintaining proper cellular function [32].

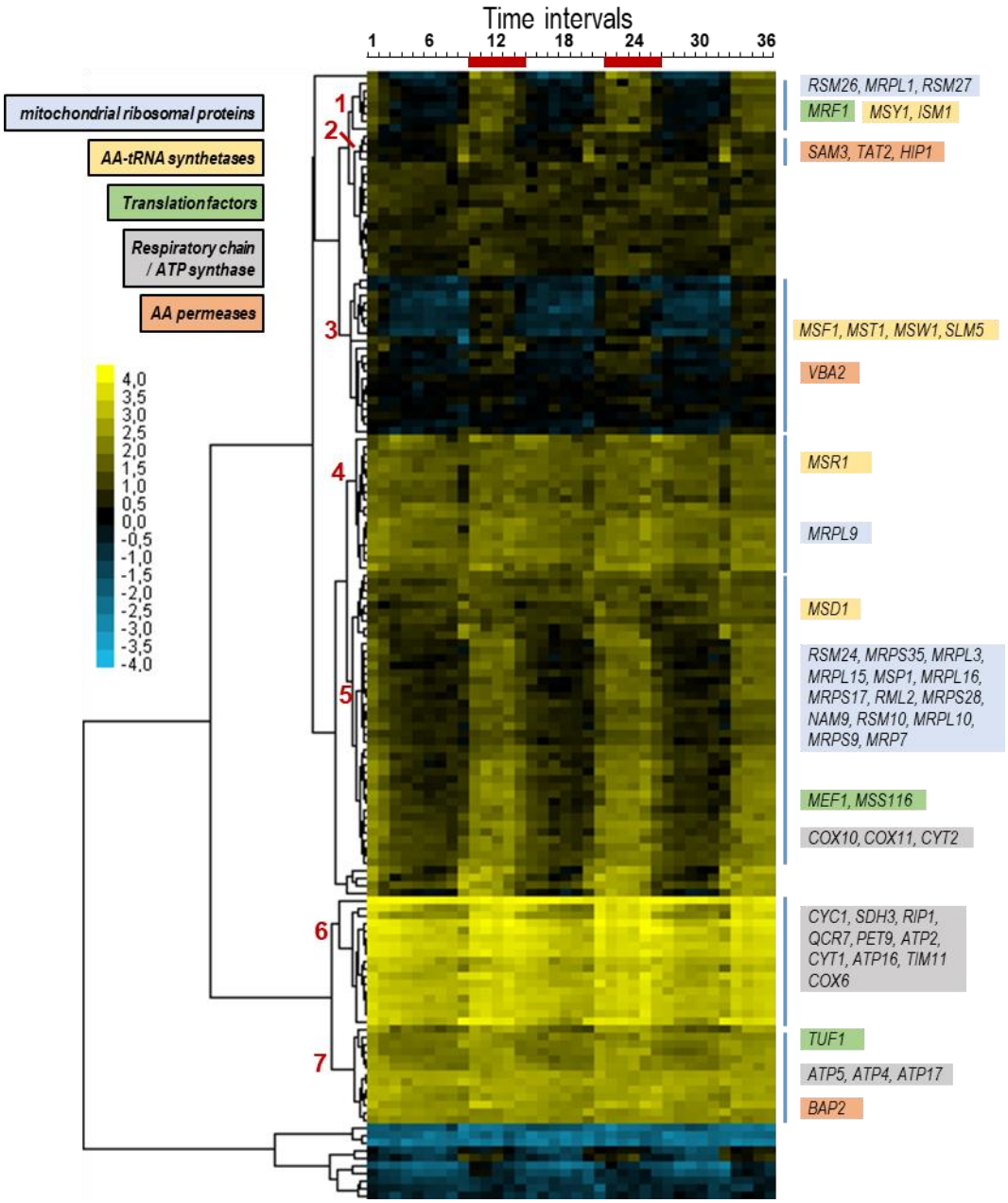

Fig. 6 Periodic profile of genes specifically induced at the pH 6.0 to 7.1 transition. Our list of 174 genes was crossed with the expression data provided by Tu and coworkers [48] which described the cyclic expression profile of yeast cells grown under continuous, nutrient limiting conditions. The data for the 149 genes common to both datasets was clustered with the Cluster 3.0 software (Euclidean distance, average linkage) [53] and plotted with JavaTreeView [54]. The numbers on the left identify the main clusters, with relevant genes shown on the right according the indicated functional colour code. Time intervals at the top correspond to the interval of sampling (approximately 25 min). The red bars show the time intervals corresponding to the reductive/building (R/B) period (see main text).

4. Material and Methods

4.1. Yeast strains and storage conditions

The *S. cerevisiae* strains used in this study are listed in **Table 1**. For prolonged storage, the strains were grown at 30 °C, 200 rpm, in YPD (1 % (w/v) yeast extract, 1 % (w/v) peptone and 2 % (w/v) glucose) medium. After overnight growth, glycerol was added to a final concentration of 30 % (v/v) and 1 mL aliquots were stored at – 80 °C.

Table 1 - List of the strains used in this work.

Strain	Genotype	Reference/source
Ace55	*W303-1A JEN1::GFP::KanMX leu2 ura3 trp1 his3 ade2*	Our laboratory collection
CENPK113-7D	MATa MAL2-8c SUC2	[55]
CB191	CENPK113-7D *JEN1::GFP::KanMX*	This work
CB270	CENPK113-7D *JEN1::GFP::HygMX*	This work

4.2. Strain construction

All the *S. cerevisiae* strains generated in this work were constructed as follows: firstly, DNA fragments were amplified by PCR (Accuzyme DNA Polymerase, Bioline, or Supreme NZYProof DNA Polymerase, Nzytech) with specific oligonucleotides (listed in **Table 2**) using yeast genomic DNA or plasmid DNA. The resulting PCR products were introduced in *S. cerevisiae* cells, by following the polyethylene glycol (PEG)/lithium acetate (LiAc) protocol [56], and the resulting transformants were selected on geneticin (G418 disulfate, J62671) or hygromycin B (Alfa Aesar; J60681) according to the resistance (R) marker present (geneticin for *kan*R and hygromycin for *hyg*R).

Specifically, the strain CB191 (**Table 1**) was obtained as following: the DNA cassette *JEN1::GFP::kanMX* was PCR amplified from the genomic DNA of the strain Ace55 (**Table 1**) with the primers W303fw and W303rev. The DNA cassette was then introduced in the CENPK113-7D strain and positive transformants were confirmed by colony PCR using the primers K3 fw and W303rev or W303fw and K2 rev.

The CB270 strain (**Table 1**) was obtained by replacing the kanamycin resistance (*kanR) sequence* by the hygromycin resistance (*hygR)* DNA region in the CB191 strain. In detail, the *hygR* DNA sequence was first amplified from pAG32 plasmid [57] using primers 150_MX4fwd and 149_MX4rev (**Table 2**), which align 50 bps before the end of TEF promoter and 50 bps after the beginning of TEF terminator, respectively.

Since KanR sequence is also flanked by TEF promoter and terminator regions, the 50 bp homology arms facilitate homologous recombination, allowing the replacement of *kanR* with *hygR*. Positive transformants were confirmed by colony PCR using primers 150 and 324. The strain CB270 (CENPK113-7D *JEN1::GFP::HygMX*) was used in all the subsequent chemostate experiments in this study.

Table 2 - List of the primers used in this work.

Primer name	Sequence (5´→ 3´)
W303fw	GATTTGTCCTCTCCTGTTATGAAG
W303rev	ATCTTGCTAGTCTTAACGGCTGTTA
K3 fw	CCATCCTATGGAACTGCCTC
K2 rev	CGATAGATTGTCGCACCTG
150_MX4fwd	AAAATCTTGCTAGGATACAGTTCTC
149_MX4rev	ACAAATGACAAGTTCTTGAAAACAA
324_Hygrev	TGCATCATCGAAATTGCCGTCAACCAA

4.3. Media and cultivation conditions

For batch cultivations, *S. cerevisiae* precultures were grown aerobically at 30 °C, 200 rpm, in 500 mL Erlenmeyer flasks containing 100 mL of synthetic medium (SM) [58] supplemented with 20 g/L of glucose. Glucose and filter-sterilized vitamins were added after autoclaving the other constituents of SM.

Continuous cultures were carried out in 2 L laboratory bioreactors (Getinge Applikon, Delft, The Netherlands) with a 1 L working volume. Cultures were grown aerobically at 30 °C, 800 rpm, in synthetic medium (for more details see [43, 58] and **Table S7**) with 33 mM (≈2.9 gL^{-1}) lactate and 50 mM (≈2.3 gL^{-1}) ethanol as sole carbon-limited sources. Ethanol and filter-sterilized vitamins (**Table S7** and [58]) were added after autoclaving the medium. After the batch phase, the medium pumps were switched on, resulting in the continuous addition of 70 mL/h of SM, supplemented with 33 mM lactate and 50 mM ethanol, to the culture. The working volume (1.0 L) was kept constant using an effluent pump controlled by an electric level sensor, resulting in a dilution rate (D) of 0.07 h^{-1}. The culture pH was maintained at 6.0, 6.5, 7.0, 7.1 or 7.2 by automated addition of 2 M KOH or 2 M H_2SO_4. Chemostat cultures were considered to be in steady-state (SS) when, after at least 5 volume changes, the culture dry weight, extracellular metabolite concentrations, the CO_2 production and O_2 consumption rates did not differ more than 5 % over 2 volume changes. The chemostat

runs were limited to less than 15-20 volume changes, after inoculation, to avoid evolutionary adaptation of the cultures.

For the pH ramp experiments, steady-state cultures were firstly established at pH 6.5 and then, a pH ramp, from pH 6.5 to pH 7.5, was programmed in which the medium pH was automatically increased over time (0.02 units per hour). The off-gas signal (CO_2 concentration) and optical density were also automatically monitored in the course of the experience. Samples for dry weight, HPLC (for external metabolites analysis) and fluorescence microscopy (to follow the cellular localization of Jen1-GFP) were taken overtime (in each pH increase of ± 0.5 units).

The cultures were independently performed at least in duplicate (n≥2).

4.4. Analytical methods

4.4.1. Optical density

Optical density at 660 nm was manually measured using a Jenway 7200 spectrophotometer (Bibby Scientific, Staffordshire, UK).

4.4.2. Off-gas

Off-gas was first cooled in a condenser at 2 °C and then dried with a Perma Pure Dryer (Permapure, Toms River, NJ). Subsequently, CO_2 and O_2 concentrations were measured using an NGA 2000 Rosemount gas analyser (Emerson, St Louis, MO, USA).

4.4.3. Dry weight

Culture dry weights were determined by filtrating 10 mL of culture using dry-, pre-weighed nitrocellulose filters with a pore size of 0.45 µm (Gelman Laboratory, Ann Arbor, MI, USA). The filters were washed twice with demineralized water before and after the filtration of the culture samples. After filtration, the filters were dried in a microwave for 20 min at 360 W and weighed again. Final dry weights are the average of duplicates performed for each chemostat culture.

4.5. High performance liquid chromatography (HPLC)

The extracellular metabolites and/or substrates present in the culture supernatants and media were analyzed by HPLC using an Agilent 1260 HPLC, equipped with a Bio-Rad HPX 87H column. For sampling steady state cultures, ≈5 mL of culture broth from the bioreactor was rapidly sampled into a syringe containing

pre-cooled stainless steel balls (4 mm, Fabory Laman Zoetermeer). The supernatant was immediately separated from the cells by filtration through a 0.45-µm pore size filter (PVD membrane, Merck Millipore Ltd.) ((adapted from [59]).

4.6. Epifluorescence microscopy and quantifications

For the detection of Jen1-GFP cellular localization, a volume of 1 mL culture was collected and concentrated by a factor of 100 by centrifugation (5000 rpm,1 min). 4 µL of each sample was then directly and immediately visualized, without fixation, on a Zeiss Axio Imager Z1 microscope (Carl Zeiss AG, Oberkochen, Germany) with appropriate filters using a 100x magnification objective.

The quantification of the ratio between the fluorescence at the cell periphery and the total fluorescence (n≥300 cells) was performed using ImageJ software (version 1.53k) as described in [18, 60]. An ordinary one-way ANOVA analysis was used followed by a Tukey´s multiple comparisons test using Prism 9.0 (GraphPad software, version 9.2.0). The *P* values are indicated (NS: $P>0.05$; *, $P<0.05$; **, $P<0.01$; ***, $P<0.001$; ****, $P<0.0001$).

4.7. RNA extraction, sequencing and analysis

4.7.1. Culture sample collection

Steady state culture samples (± 240 mg of cells) were collected directly from the bioreactor and instantaneously frozen in liquid nitrogen and stored at – 80 °C for further RNA sample extraction.

4.7.2. RNA extraction

For RNA extraction, ≈ 800 µL of “crushed ice” bits, from the – 80 °C samples, were transferred to Eppendorf tubes and thawed on ice. Eppendorfs were then centrifuged at 8000 *g*, 4 min, 0 °C and the pellet was resuspended in 200 µL cold RNase-free water. Subsequently, 400 µL of acid phenol-chloroform was quickly added and the mixture was centrifuged at 8000 *g*, for 4 min, at room temperature. The aqueous layer was transferred to a new tube and 400 µL of chloroform was added. The mixture was centrifuged again at 8000 *g*, 4 min, room temperature, and the upper layer was transferred to a new tube. 20 µL of 3 M Na-acetate and 500 µL of 100 % (v/v) ethanol (– 20 °C) were added. After mix by vortexing, the samples were incubated at – 20 °C for at least 15 min. The samples were then centrifuged for 15 min, 4°C, at

8000 *g* and the pellet was washed with 500 µL 80 % (v/v) ethanol (– 20 °C). The samples were vortexed, centrifuged again and, after removal of all the ethanol, the pellet was resuspended in 20 µL RNase-free water. The samples were kept at room temperature for at least 2 h to dissolve the RNA. The concentration, purity and quality of the total RNA samples were also determined using Tapestation (Agilent Technologies 2200) and NanoDrop 2000 (Thermo scientific).

4.7.3. RNA sequencing

RNA samples [8 samples, four different pHs (6.0; 6.5; 7.0 and 7.1) in duplicate] were sent to Novogene (UK) for mRNA sequencing (RNA-seq).

4.7.4. Analysis of RNA-Seq data

Mapping of paired-end clean reads (2x150 nt) were aligned to the *S. cerevisiae* CEN.PK113-7D genome (assembly ASM26988v1, obtained from https://fungi.ensembl.org/) with the Hisat2 v2.0.5 software [61]. Percentages of overall alignment were between 92 and 98%. The featureCounts (v1.5.0-p3) program was used to count the number of reads mapped to each gene. Differential expression analysis was conducted using DESeq2 R package (1.20.0) using the Benjamini and Hochberg's approach to adjust the resulting P-values [62]. Genes with an adjusted P-value <=0.01 found by DESeq2 and a log(2) fold change of +/- 0.6 were assigned as differentially expressed. Gene Ontology analyses for functional profiling were done with the g.Profiler server (https://biit.cs.ut.ee/ gprofiler/gost) using *S. cerevisiae* data. The search for transcription factors binding sites in the promoters of the selected genes was carried out at the Regulatory Sequence Analysis Tools (RSAT) server (https://rsat.france-bioinformatique.fr/fungi/) with the matrix-scan tool [63] and selecting an upstream segment of 800 nt (allowing overlapping with ORF). The transcription factor matrix data from the JASPAR database [64] was used and a *p*-value of 10^{-4} was set as significance threshold. Four individual sets of 174 promoters randomly extracted were also analysed and used as reference.

RNA-Seq data was deposited at *Repositório de Dados da Universidade do Minho* (dataRepositóriUM) under study https://doi.org/10.34622/datarepositorium/LWNKLQ.

5. Acknowledgments

We thank Marieke Warmerdam (TU Delft) and Charlotte Koster (TU Delft) for assistance and help in some of the laboratory experiments. We are also grateful to George Diallinas (University of Athens) for the critical reading of this manuscript.

6. Funding

This work was supported by the MetaFungal project PTDC/BIA-MIC/5246/2020 (http://doi.org/10.54499/PTDC/BIA-MIC/5246/2020) through the 'Fundação para a Ciência e a Tecnologia' (FCT). Work at University of Minho (CBMA) was supported by the 'Contrato-Programa' UIDB/04050/2020 (https://doi.org/10.54499/UIDB/04050/2020) and the Contrato-Programa" LA/P/0069/2020 (https://doi.org/10.54499/LA/P/0069/2020) funded by national funds through the FCT I.P. Work at UAB was funded by grant number PID2020-113319RB-I00 (MCIN/AEI/10.13039/501100011033, Ministerio de Ciencia e Innovación, Spain) to JA. C.B.-A. acknowledges FCT for the PhD grants PD/BD/135208/2017 and COVID/BD/152003/2021 (https://doi.org/10.54499/COVID/BD/152003/2021) and FEBS for the Short-Term Fellowship (September 1 to November 1st, 2021) to support her stay at TU Delft University.

7. Conflict of Interest

The authors declare that they have no interest or financial conflicts with the contents of this article.

8. Supporting Information

This article contains supporting information.

9. References

1. Zaman S, Lippman SI, Zhao X, Broach JR (2008) How Saccharomyces responds to nutrients. Annu Rev Genet 42:27–81. https://doi.org/10.1146/annurev.genet.41.110306.130206
2. Dikicioglu D, Karabekmez E, Rash B, et al (2011) How yeast re-programmes its transcriptional profile in response to different nutrient impulses. BMC Syst Biol 5:148. https://doi.org/10.1186/1752-0509-5-148
3. Taymaz-Nikerel H, Cankorur-Cetinkaya A, Kirdar B (2016) Genome-Wide Transcriptional Response of Saccharomyces cerevisiae to Stress-Induced Perturbations. Front Bioeng Biotechnol 4:17. https://doi.org/10.3389/fbioe.2016.00017
4. Estruch F (2000) Stress-controlled transcription factors, stress-induced genes and stress tolerance in budding yeast. FEMS Microbiol Rev 24:469–486. https://doi.org/10.1111/j.1574-6976.2000.tb00551.x
5. Barata-Antunes C, Alves R, Talaia G, et al (2021) Endocytosis of nutrient transporters in fungi: The ART of connecting signaling and trafficking. Comput Struct Biotechnol J 19:1713–1737. https://doi.org/10.1016/j.csbj.2021.03.013
6. Babst M (2020) Regulation of nutrient transporters by metabolic and environmental stresses. Curr Opin Cell Biol 65:35–41. https://doi.org/10.1016/j.ceb.2020.02.009
7. Babst M (2014) Quality control at the plasma membrane: One mechanism does not fit all. J Cell Biol 205:11–20. https://doi.org/10.1083/jcb.201310113
8. Cassio F, Leao C, Van Uden N (1987) Transport of lactate and other short-chain monocarboxylates in the yeast Saccharomyces cerevisiae. Appl Environ Microbiol 53:509–513. https://doi.org/10.1128/aem.53.3.509-513.1987
9. Casal M, Paiva S, Andrade RP, et al (1999) The lactate-proton symport of Saccharomyces cerevisiae is encoded by JEN1. J Bacteriol 181:2620–3. https://doi.org/10.1128/JB.181.8.2620-2623
10. Soares-Silva I, Schuller D, Andrade RP, et al (2003) Functional expression of the lactate permease Jen1p of Saccharomyces cerevisiae in Pichia pastoris. Biochem J 376:781–787. https://doi.org/10.1042/BJ20031180
11. Soares-Silva I, Paiva S, Diallinas G, Casal M (2007) The conserved sequence NXX[S/T]HX[S/T]QDXXXT of the lactate/pyruvate:H(+) symporter subfamily defines the function of the substrate translocation pathway. Mol Membr Biol 24:464–74. https://doi.org/10.1080/09687680701342669
12. McDermott JR, Rosen BP, Liu Z (2010) Jen1p: A High Affinity Selenite Transporter in Yeast. Mol Biol Cell 21:3934–3941. https://doi.org/10.1091/mbc.E10-06-0513
13. Andrade RP, Casal M (2001) Expression of the lactate permease gene JEN1 from the yeast Saccharomyces cerevisiae. Fungal Genet Biol 32:105–111. https://doi.org/10.1006/fgbi.2001.1254
14. Paiva S, Kruckeberg AL, Casal M (2002) Utilization of green fluorescent protein as a marker for studying the expression and turnover of the monocarboxylate permease Jen1p of Saccharomyces cerevisiae. Biochem J 363:737–744. https://doi.org/10.1042/0264-6021:3630737
15. Paiva S, Vieira N, Nondier I, et al (2009) Glucose-induced ubiquitylation and endocytosis of the yeast Jen1 transporter: role of lysine 63-linked ubiquitin chains. J Biol Chem 284:19228–36. https://doi.org/10.1074/jbc.M109.008318
16. Becuwe M, Herrador A, Haguenauer-Tsapis R, et al (2012) Ubiquitin-mediated regulation of endocytosis by proteins of the arrestin family. Biochem Res Int

2012:1–12. https://doi.org/10.1155/2012/242764
17. Becuwe M, Léon S (2014) Integrated control of transporter endocytosis and recycling by the arrestin-related protein Rod1 and the ubiquitin ligase Rsp5. Elife 3:1–23. https://doi.org/10.7554/eLife.03307
18. Hovsepian J, Albanèse V, Becuwe M, et al (2018) The yeast arrestin-related protein Bul1 is a novel actor of glucose-induced endocytosis. Mol Biol Cell 33:1012–1020. https://doi.org/10.1091/mbc.E17-07-0466
19. Fujita S, Sato D, Kasai H, et al (2018) The C-terminal region of the yeast monocarboxylate transporter Jen1 acts as a glucose signal-responding degron recognized by the α-arrestin Rod1. J Biol Chem 293:10926–10936. https://doi.org/10.1074/jbc.RA117.001062
20. Barata-Antunes C, Talaia G, Broutzakis G, et al (2022) Interactions of cytosolic tails in the Jen1 carboxylate transporter are critical for trafficking and transport activity. J Cell Sci. https://doi.org/10.1242/jcs.260059
21. Talaia G, Gournas C, Saliba E, et al (2017) The α-Arrestin Bul1p Mediates Lactate Transporter Endocytosis in Response to Alkalinization and Distinct Physiological Signals. J Mol Biol 429:3678–3695. https://doi.org/10.1016/j.jmb.2017.09.014
22. ter Linde JJ, Liang H, Davis RW, et al (1999) Genome-wide transcriptional analysis of aerobic and anaerobic chemostat cultures of Saccharomyces cerevisiae. J Bacteriol 181:7409–7413. https://doi.org/10.1128/JB.181.24.7409-7413.1999
23. Hoskisson PA, Hobbs G (2005) Continuous culture-making a comeback? Microbiology 151:3153–3159. https://doi.org/10.1099/mic.0.27924-0
24. Mitchell P (1966) Chemiosmotic coupling in oxidative and photosynthetic phosphorylation. Biol Rev Camb Philos Soc 41:445–502. https://doi.org/10.1111/j.1469-185x.1966.tb01501.x
25. Maris AJAV, Konings WN, Dijken JPV, Pronk JT (2004) Microbial export of lactic and 3-hydroxypropanoic acid: Implications for industrial fermentation processes. Metab Eng 6:245–255. https://doi.org/10.1016/j.ymben.2004.05.001
26. Porro D, Bianchi M, Ranzi B, et al (1999) Yeast strains for the production of lactic acid. 1–86
27. Branduardi P, Sauer M, De Gioia L, et al (2006) Lactate production yield from engineered yeasts is dependent from the host background, the lactate dehydrogenase source and the lactate export. Microb Cell Fact 5:1–12. https://doi.org/10.1186/1475-2859-5-4
28. Pacheco A, Talaia G, Sá-Pessoa J, et al (2012) Lactic acid production in Saccharomyces cerevisiae is modulated by expression of the monocarboxylate transporters Jen1 and Ady2. FEMS Yeast Res 12:375–381. https://doi.org/10.1111/j.1567-1364.2012.00790.x
29. Wakamatsu M, Tomitaka M, Tani T, et al (2013) Improvement of ethanol production from D-lactic acid by constitutive expression of lactate transporter Jen1p in Saccharomyces cerevisiae. Biosci Biotechnol Biochem 77:1114–1116. https://doi.org/10.1271/bbb.120985
30. Peña A, Cinco G, Gómez-Puyou A, Tuena M (1972) Effect of the pH of the incubation medium on glycolysis and respiration in Saccharomyces cerevisiae. Arch Biochem Biophys 153:413–425. https://doi.org/10.1016/0003-9861(72)90359-1
31. Orij R, Postmus J, Ter Beek A, et al (2009) In vivo measurement of cytosolic and mitochondrial pH using a pH-sensitive GFP derivative in Saccharomyces

cerevisiae reveals a relation between intracellular pH and growth. Microbiology 155:268–278. https://doi.org/10.1099/mic.0.022038-0

32. Orij R, Brul S, Smits GJ (2011) Intracellular pH is a tightly controlled signal in yeast. Biochim Biophys Acta 1810:933–944. https://doi.org/10.1016/j.bbagen.2011.03.011
33. Orij R, Urbanus ML, Vizeacoumar FJ, et al (2012) Genome-wide analysis of intracellular pH reveals quantitative control of cell division rate by pH(c) in Saccharomyces cerevisiae. Genome Biol 13:R80. https://doi.org/10.1186/gb-2012-13-9-r80
34. Weusthuis RA, Pronk JT, Van Den Broek PJA, Van Dijken JP (1994) Chemostat cultivation as a tool for studies on sugar transport in yeasts. Microbiol Rev 58:616–630. https://doi.org/10.1128/mmbr.58.4.616-630.1994
35. Liu Z, Butow RA (1999) A transcriptional switch in the expression of yeast tricarboxylic acid cycle genes in response to a reduction or loss of respiratory function. Mol Cell Biol 19:6720–6728. https://doi.org/10.1128/MCB.19.10.6720
36. Broach JR (2012) Nutritional control of growth and development in yeast. Genetics 192:73–105. https://doi.org/10.1534/genetics.111.135731
37. Jazwinski SM (2013) The retrograde response: when mitochondrial quality control is not enough. Biochim Biophys Acta 1833:400–409. https://doi.org/10.1016/j.bbamcr.2012.02.010
38. Buschlen S, Amillet J-M, Guiard B, et al (2003) The S. Cerevisiae HAP complex, a key regulator of mitochondrial function, coordinates nuclear and mitochondrial gene expression. Comp Funct Genomics 4:37–46. https://doi.org/10.1002/cfg.254
39. Mao Y, Chen C (2019) The Hap Complex in Yeasts: Structure, Assembly Mode, and Gene Regulation. Front Microbiol 10:1645. https://doi.org/10.3389/fmicb.2019.01645
40. Turcotte B, Liang XB, Robert F, Soontorngun N (2010) Transcriptional regulation of nonfermentable carbon utilization in budding yeast. FEMS Yeast Res 10:2–13. https://doi.org/10.1111/j.1567-1364.2009.00555.x
41. Akita O, Nishimori C, Shimamoto T, et al (2000) Transport of pyruvate in Saccharomyces cerevisiae and cloning of the gene encoded pyruvate permease. Biosci Biotechnol Biochem 64:980–984. https://doi.org/10.1271/bbb.64.980
42. Casal M, Paiva S, Queirós O, Soares-Silva I (2008) Transport of carboxylic acids in yeasts. FEMS Microbiol Rev 32:974–994. https://doi.org/10.1111/j.1574-6976.2008.00128.x
43. Verduyn C, Postma E, Scheffers WA, van Dijken JP (1990) Physiology of Saccharomyces cerevisiae in anaerobic glucose-limited chemostat cultures. J Gen Microbiol 136:395–403. https://doi.org/10.1099/00221287-136-3-395
44. Wasungu KM, Simard RE (1982) Growth characteristics of bakers' yeast in ethanol. Biotechnol Bioeng 24:1125–1134. https://doi.org/10.1002/bit.260240509
45. Lamb TM, Xu W, Diamond A, Mitchell AP (2001) Alkaline response genes of Saccharomyces cerevisiae and their relationship to the RIM101 pathway. J Biol Chem 276:1850–1856. https://doi.org/10.1074/jbc.M008381200
46. Serrano R, Ruiz A, Bernal D, et al (2002) The transcriptional response to alkaline pH in Saccharomyces cerevisiae: evidence for calcium-mediated signalling. Mol Microbiol 46:1319–1333. https://doi.org/10.1046/j.1365-2958.2002.03246.x
47. Casamayor A, Serrano R, Platara M, et al (2012) The role of the Snf1 kinase in

the adaptive response of Saccharomyces cerevisiae to alkaline pH stress. Biochem J 444:39–49. https://doi.org/10.1042/BJ20112099

48. Tu BP, Kudlicki A, Rowicka M, McKnight SL (2005) Logic of the yeast metabolic cycle: temporal compartmentalization of cellular processes. Science 310:1152–1158. https://doi.org/10.1126/science.1120499
49. Serra-Cardona A, Canadell D, Ariño J (2015) Coordinate responses to alkaline pH stress in budding yeast. Microb Cell 2:182–196. https://doi.org/10.15698/mic2015.06.205
50. Heyland J, Fu J, Blank LM (2009) Correlation between TCA cycle flux and glucose uptake rate during respiro-fermentative growth of Saccharomyces cerevisiae. Microbiology 155:3827–3837. https://doi.org/10.1099/mic.0.030213-0
51. Moharir A, Gay L, Appadurai D, et al (2018) Eisosomes are metabolically regulated storage compartments for APC-type nutrient transporters. Mol Biol Cell 29:2113–2127. https://doi.org/10.1091/mbc.E17-11-0691
52. De Kok S, Kozak BU, Pronk JT, Van Maris AJA (2012) Energy coupling in Saccharomyces cerevisiae: Selected opportunities for metabolic engineering. FEMS Yeast Res 12:387–397. https://doi.org/10.1111/j.1567-1364.2012.00799.x
53. de Hoon MJL, Imoto S, Nolan J, Miyano S (2004) Open source clustering software. Bioinformatics 20:1453–1454. https://doi.org/10.1093/bioinformatics/bth078
54. Saldanha AJ (2004) Java Treeview--extensible visualization of microarray data. Bioinformatics 20:3246–3248. https://doi.org/10.1093/bioinformatics/bth349
55. Nijkamp JF, van den Broek M, Datema E, et al (2012) De novo sequencing, assembly and analysis of the genome of the laboratory strain Saccharomyces cerevisiae CEN.PK113-7D, a model for modern industrial biotechnology. Microb Cell Fact 11:1–16. https://doi.org/10.1186/1475-2859-11-36
56. Gietz RD, Woods RA (2002) Transformation of yeast by lithium acetate/single-stranded carrier DNA/polyethylene glycol method. Methods Enzymol 350:87–96
57. Goldstein AL, McCusker JH (1999) Three new dominant drug resistance cassettes for gene disruption in Saccharomyces cerevisiae. Yeast 15:1541–1553. https://doi.org/10.1002/(SICI)1097-0061(199910)15:14<1541::AID-YEA476>3.0.CO;2-K
58. Verduyn C, Postma E, Scheffers WA, van Dijken JP (1992) Effect of Benzoic Acid on Metabolic Fluxes in Yeasts: Yeast 8:501–517
59. Mashego MR, van Gulik WM, Vinke JL, Heijnen JJ (2003) Critical evaluation of sampling techniques for residual glucose determination in carbon-limited chemostat culture of Saccharomyces cerevisiae. Biotechnol Bioeng 83:395–399. https://doi.org/10.1002/bit.10683
60. Barata-Antunes C, Talaia G, Broutzakis G, et al (2021) Interactions of cytosolic termini of the Jen1 monocarboxylate transporter are critical for trafficking, transport activity and endocytosis
61. Kim D, Paggi JM, Park C, et al (2019) Graph-based genome alignment and genotyping with HISAT2 and HISAT-genotype. Nat Biotechnol 37:907–915. https://doi.org/10.1038/s41587-019-0201-4
62. Love MI, Huber W, Anders S (2014) Moderated estimation of fold change and dispersion for RNA-seq data with DESeq2. Genome Biol 15:550. https://doi.org/10.1186/s13059-014-0550-8
63. Santana-Garcia W, Castro-Mondragon JA, Padilla-Gálvez M, et al (2022) RSAT

2022: regulatory sequence analysis tools. Nucleic Acids Res 50:W670–W676. https://doi.org/10.1093/nar/gkac312

64. Castro-Mondragon JA, Riudavets-Puig R, Rauluseviciute I, et al (2022) JASPAR 2022: the 9th release of the open-access database of transcription factor binding profiles. Nucleic Acids Res 50:D165–D173. https://doi.org/10.1093/nar/gkab1113